Regional Ionosphere Mapping Using Zero Difference GPS Carrier Phase

Heba Tawfeek[1], Ahmed Sedeek[2], Mostafa Rabah[3], Gamal El-Fiky[1]

1. Faculty of Engineering, Zagazig University, Egypt,
2. Higher Institute of Engineering and Technology, El-Behira, Egypt,
3. Benha Faculty of Engineering, Benha University, Egypt.

الملخص العربى

النشاط الأيونوسفيري، يمكن استخلاصه من إشارات GNSS ذات التردد المزدوج، ثم تحويلها إلى المحتوي الإلكتروني الكلي العمودي (VTEC) على طول مسار الإشارة. وقد وضعت نماذج مختلفة لحساب VTEC. ومن أمثلة هذه النماذج نموذج الدالة متعدد الحدود وتحليل التوافقات الكروية. الفرضية الشائعة لهذه النماذج هي أنها مبنية على افتراض أن محتوى الإلكترون بأكمله في الأيونوسفير يتركز في شريحة رقيقة واحدة عند ارتفاع محدد فوق الأرض. ونظرا لعدم وجود خدمة GNSS الدولية (محطات IGS) على شمال أفريقيا، وخاصة على مصر، يتم عرض البحث الحالي لتقديم نموذج قادر على إنتاج خرائط VTEC الإقليمية على أساس كل ساعتين. ويوضح هذا البحث المفهوم والأمثلة العملية لتخطيط الأيونوسفير الآني. وقد استندت النموذج المقدم إلى صفر الاختلاف للطور فى النشاط الأيونوسفيري المسمى (ZDPID). تم تطبيق نموذج جديد لحل الغموض لموجات GPS باستخدام متسلسلة أقل تعديل مربع (SLS) لتثبيت موجات الغموض لكل ظهور للقمر. تم كتابة النموذج المقترح باستخدام كود ماتلاب. لاختبار وتقييم النموذج المقدم، تم حساب قيم VTEC على محطتين من (IGS)، وهما ANKR و BSHM. تم مقارنة نتائج النموذج مع خرائط الأيونوسفير العالمية (GIMs)، والتي تستخدم عادة كمرجع. ZDPID. يعطي الكثير صورة أكثر تفصيلا والإدراك الحقيقي للخريطة الأيونوسفير المحلية من نقطة واحدة. واستخدمت ثلاث محطات GPS أخرى في مصر لتوليد خرائط الأيونوسفير الإقليمية على دلتا النيل، مصر. قد اثبتت النتائج أن النموذج المقترح قادر على تقدير VTEC بكفاءة.

Abstract

Ionospheric delay, can be derived from dual frequency GNSS signals, and then converted into the Vertical Total Electron Contents (VTEC) along the signal path. Various models were devised to calculate VTEC. Examples of such models are the polynomial function model and spherical harmonics analysis. A common hypothesis of these models is that they are constructed based on the assumption that the entire electron content in the ionosphere is concentrated in a single thin shell at a selected height above Earth. Due to the lack of International GNSS Service (IGS stations) over the North Africa, especially over Egypt, the current paper is presented to introduce an algorithm able to produce regional TEC maps on an hourly basis. This paper demonstrates the concept and practical examples of instantaneous ionosphere mapping, based on GPS carrier phase observations using dual frequency GPS observations over Nile Delta. The developed algorithm was based on Zero-

differenced phase Ionospheric Delay (ZDPID). A concept for GPS phase ambiguity resolution model was applied using Sequential Least Square Adjustment (SLSA) to fix ambiguity term in phase observations. The proposed algorithm was written using MATLAB code and Called (ZDPID). To test and evaluate the developed code, TEC values were estimated over two stations from the (IGS), namely ANKR and BSHM. Results of the introduced algorithm are compared to the Global Ionosphere Maps (GIMs), which is generally used as a reference. The results show that the mean difference between VTEC from GIM and estimated VTEC at ANKR station is ranging from -2.1 to 3.67 TECU and The mean difference between VTEC from GIM and estimated VTEC at BSHM station is ranging from -0.29 to 3.65 TECU. ZDPID gives a much more detailed picture and real perception of the local ionosphere map from single point. Another three GPS stations in Egypt were used to generate regional ionosphere maps over Nile Delta, Egypt. The mean TEC value of IGS GIM is higher than the three stations at the most time. The difference rang between IGS GIM and SAID station is from - 1.1 to 3.69 TECU, from -1.29 to 3.27 TECU for HELW station, and from 0.2 to 4.2 TECU for BORG station. The results of the proposed algorithm are able to estimate TEC efficiently.

1. Introduction

Global Navigation Satellite Systems (GNSS), are considered as important cost-effective tools to remotely sense the Earth's ionosphere and investigate its characteristics. This is due to the global system coverage and multiple frequency data available via a world-wide network of GPS stations. Since the ionosphere is a dispersive medium, this multiple frequency data can be used to derive the integrated measurements of electron density, which is known as *TEC*, along the line-of sight between a given satellite and receiver. By estimating *VTEC* values from a network of dual frequency GPS receivers, useful information about the ionosphere can be derived. Dual-frequency GPS receivers demonstrate the number of electrons in the ionosphere layer in a column of 1 m^2 cross-section.It is called the Slant Total Electron Content (*STEC*) which is extending along the ray-path of the signal between the satellite and the receiver.

Various methods were devised to calculate the ionospheric delay and *STEC*. These methods were based on spherical harmonic expansions in the global or regional and station scale (e.g. Schaer, 1999, and Wielgosz et al., 2003a). Local methods were based on two-dimensional Taylor series expansions (e.g. Komjathy, 1997, Jakobsen et al. 2010, Deng et al 2009, and Masaharu et al. 2013). A commonly used model is the grid model where the area being modeled is represented by fixed grid points in latitude and longitude. In this

model, *TEC* values are mapped to a single ionospheric shell at fixed altitude where the maximum electron density is assumed to occur (normally a value in the range 250-400 km).

The GPS receivers use the C/A and P codes to determine the pseudo range, which is a measure of the distance between the satellite and the receiver, as the electromagnetic signal travels at the speed of light, the pseudo range can be computed by simply multiplying the time offset by the speed of light. The precision for the pseudo range measurements has been traditionally about 1% of their chip lengths, which corresponds to a precision of roughly 3 m for C/A code measurements and 0.3 m for P-code measurements (Hofmann-Wellenhof et al., 2008). GPS receiver can measure the phase of the carrier wave and track the changes in the phase but the whole number of carrier cycles that lie between the satellite and the receiver is initially unknown. To use the carrier phase as an observable for estimating ionospheric error, this unknown number of cycles or ambiguity, *N*, has to be determined with appropriate methods (Langley, 1998).

Ionospheric mapping is defined as a technique applying simultaneously measured TEC values to generate VTEC maps referred to a specific time epoch (Stanislawska et. al. 2000). Several studies have been performed for regional ionosphere mapping (Wielgosz et. al. 2003b; Nohutcu et. al. 2010; Salih Alcay et al. 2012). There are several groups which are capable of producing regional and/or global ionospheric maps like IGS Processing Center at the Astronomical Institute of the University of Bern, the Orbit Attitude Division of the European Space Operations Centre, and At the GPS Network and Operations Group of the Jet Propulsion Laboratory, the stations from the IGS network are using to produce regional and global ionospheric maps (Feltens et al., 1996). Regional ionospheric maps are routinely produced and made available on the Internet (Sardon et al., 1995; Jakowski et al., 1996).

Due to the lack of GPS stations over the equatorial, North Africa and Atlantic in IGS network, we suggested the proposed algorithm to be able to produce ionospheric maps over Egypt and over any other GPS station accurately. Therefore, the Ionospheric activity over Nile Delta, Egypt, was investigated using three GPS stations. The GPS data used here are from regional GPS reference observed by National Research Institute of Astronomy and Geophysics (NRIAG).

The introduced new algorithm in this study is based upon utilizing dual frequency GPS carrier phase observation because of its high precision to produce Ionospheric maps using a single GPS station (Zero Differenced) under MATLAB environment. In the present paper, Sequential Least Square Adjustment (*SLSA)* is considered to fix the ambiguity term to overcome the singularity in the observation equation. To test and evaluate the proposed algorithm two stations from IGS were considered, and the resulted ionosphere maps were compared with the Global Ionosphere Maps (GIMs), which is generally used as a reference.

2. GPS Observations

The observations of dual-frequency GPS receiver*(L1* and *L2)* setup at any station consists of two codes and two carrier phase observations in RINEX format whichwere used for present model. The observations equations for pseudo-ranges and carrier-phase measurements can be formulated as follows (Leandro, 2009; Sedeek et al., 2017):

$$P1 = R + c(dT - dt) + T + I + HDr,1 - HDs,1 + M1 + E1 \qquad (1)$$

$$P2 = R + c(dT - dt) + T + \gamma I + HDr,2 - HDs,2 + M2 + E2 \qquad (2)$$

$$\Phi1 = R + c(dT - dt) + T - I + \lambda1N1 + pbr,1 - pbs,1 + hdr,1 - hds,1 + m1 + e1 \qquad (3)$$

$$\Phi2 = R + c(dT - dt) + T - \gamma I + \lambda2N2 + pbr,2 - pbs,2 + hdr,2 - hds,2 + m2 + e2 \qquad (4)$$

Where:

P1 and P2   Pseudo-range measurements on L1 and L2 frequencies, respectively, in meter;

$\Phi1$ and $\Phi2$ carrier-phase measurements on L1 and L2 frequencies, respectively, in meter;

R   the geometric distance between satellite and receiver antennas, in meters

C   the speed of light, in meters per second;

dT and dt   receiver and satellite clock errors, respectively, in seconds;

T   the neutral troposphere delay, in meters;

I   the L1 frequency ionosphere delay, in meters;

Γ the factor to convert the ionospheric delay from L1 to L2 frequency,

N1 and N2   carrier-phase integer ambiguities on L1 and L2 frequencies, respectively, in cycles;

$\lambda1$ and $\lambda2$ carrier-phase wave length on L1 and L2 frequencies, respectively, in meters;

HDr,i   and receiver and satellite pseudo-range hardware delays, respectively, in metric
HDs,i   units, where i represents the frequency (L1 or L2);

hdr,i and hds,i receiver and satellite carrier-phase hardware delays, respectively, in metric units, where i represents the frequency (L1 or L2);

M1 and M2   Pseudo-range multipath on L1 and L2 frequencies, respectively, in meters;

E1 and E2   Other un-modeled errors of pseudo-range measurements on L1 and L2 frequencies, respectively, in meters.

pbr,i and pbs,i receiver and satellite carrier-phase initial phase bias, respectively, in metric units, where i represents the carrier frequency (L1 or L2);

m1 and m2   carrier-phase multipath on L1 and L2 frequencies, respectively, in meters;

el and e2   Other un-modeled errors of carrier-phase measurements on L1 and L2 frequencies, respectively, in meters.

3. Fixing Ambiguity using Sequential Least Square

Using GPS carrier-phase measurements for estimating Ionospheric delay depends upon the ability to determine the ambiguities in the number of carrier-phase cycles. Normally, the exact integer carrier-phase ambiguities are determined to estimate Ionospheric delay.

To solve this problem, we use Ionosphere-free and Geometry-free Combinations algorithms as follows (Guochang Xu, 2004):

$$\begin{bmatrix} \lambda_1 N_1 \\ \lambda_2 N_2 \\ B1 \\ \varepsilon \end{bmatrix} = \begin{bmatrix} 1-2a & -2b & 0 & 2 \\ -2a & -2a-1 & 0 & 1 \\ 1/q & -1/q & 0 & 0 \\ a & b & 0 & 0 \end{bmatrix} \begin{bmatrix} P1 \\ P2 \\ \Phi1 \\ \Phi2 \end{bmatrix} \tag{5}$$

Where:

$$a = f_1^2/(f_1^2 - f_2^2), \quad b = -f_2^2/(f_1^2 - f_2^2), \quad q = f_1^2 * (1/f_1^2 - 1/f_2^2).$$

$\varepsilon = R + c.(dT - dt) + T + m_j + e_j, j=p;\Phi,$

$I = B1$, $B1$ is ionospheric parameters in the path and zenith,

f_i^2:Frequency where i: 1; 2.

This stage gives the solution of ambiguity term. The ionospheric delay $B1$ which would be a check of our autonomous ionospheric delay $I_{1(t_0,t_{0+n})}$ that will be defined later in eq. (13). To fix the nature of the ambiguities, we can apply Sequential Least Square Adjustment to fix the ambiguity term to be one value of all epochs of every rise of satellite. This partitioning of the observation model is represented in following forms (Guochang Xu, 2004):

$$L=AX \quad \text{and} \quad L = \begin{bmatrix} L1 \\ L2 \end{bmatrix} \quad n = \begin{bmatrix} n1 \\ n2 \end{bmatrix} \quad A = \begin{bmatrix} A1 \\ A2 \end{bmatrix} \quad P = \begin{bmatrix} P1 \\ P2 \end{bmatrix} \tag{6}$$

Where: L is the vector of observations of the ambiguity term, A is the design matrix, X is unknown parameters vector, n is the vector of unknowns and P is weight matrix of observations with size $n*n$. L_1 and L_2 are first and second groups of observations which its number n_1 and n_2. The design matrix A_1 and A_2 and its weight matrix P_1 with dimension n_1*n_1 and P_2 with dimension n_2*n_2 respectively. We suppose that n1 is the first five epochs and a preliminary solution x_o can be calculated as follows:

$x_o = (A_1{}^T P_1.A_1)^{-1} A_1{}^T.P_1. L_1$ (7)

The change due to the additional observation set L2 is denoted as $\varDelta x$:

$\varDelta x = (A_1{}^T P_1.A_1 + A_2{}^T P_2.A_2)-1. A_2{}^T P_2 (L_2 - A_2. x_o)$ (8)

$X = x_o + \varDelta x$ (9)

By using this system of equations, final float ambiguities values are computed.

4. Geometry-Free Linear Combination of GPS Observables

The geometry-free linear combination of GPS observations is classically used for ionospheric investigations and it is obtained by subtracting simultaneous pseudo range (P1-P2 or C1-P2) or carrier phase observations (Φ1-Φ2). With this combination, the satellite – receiver geometrical range and all frequency independent biases are removed (Ciraolo et al., 2007). Subtracting Eq. (3) from Eq. (4) the geometry-free linear combination for carrier phase observations is obtained (Sedeek et al, 2017):

$$L_{4(t)} =$$

$$\Phi_{GF} = \Phi_1 - \Phi_2 = (\gamma - 1) I_1 + \lambda_1 N_1 - \lambda_2 N_2 + c(\Delta hdr - \Delta hds) + \varepsilon_{(\Phi_1 - \Phi_2)}$$

(10)

Where: ε(Φ1 - Φ2) is the noise term in phase equation can be neglected for the sake of simplicity, Δhdr is the difference carrier-phase hardware delays bias between *L1* & *L2* frequency for receiver, Δhds is the difference carrier-phase hardware delays bias between *L1* & *L2* frequency for satellite, the factor γ is the factor to convert the ionospheric delay from L1 to L2 frequency

$$I_2 = \frac{40.3\ STEC}{f_2{}^2} = \frac{f_1{}^2}{f_2{}^2} I_1 = \gamma I_1, \gamma = \frac{f_1{}^2}{f_2{}^2}$$ (11)

$DCBs = C \times (\Delta hdr - \Delta hds)$ (12)   The satellite and the receiver *DCBs* are known to be the main error sources in the estimation of the total electron content (*TEC*) using GPS measurements. The *TEC* errors that resulted from *DCBs* in both the satellite and receiver can reach up to several nanoseconds (ns) (Sardon and Zarraoa 1997). So in the current study, the satellite and receiver *DCB* were taken from IGS products (ION files). L_4 at epoch (t) is the carrier phase Geometry free (Φ_{GF}) after repair cycle slips. In the present paper, Melbourne-Wübbena (1985) Linear Combination is utilized to detect and repair cycle slips. The epoch-differenced in carrier phase Geometry free(Φ_{GF}) is sufficient for estimating ionospheric delay then *VTEC* estimation, and therefore we use the epoch-difference ∂L_4 instead of L_4 itself (Araujo-Pradere et al., 2007).

$$\partial L_{4(t_0,t_{0+k})} = L_{4(t_{0+k})} - L_{4(t_0)} = \frac{f_1^2 - f_2^2}{f_1^2} \partial I_{1(t_0,t_{0+k})} \tag{13}$$

$$I_{1(t_{0+n})} = I_{1(t_0)} + \sum \partial I_{1(t_0,t_{0+n})} \tag{14}$$

Where: k is epoch number $(t_0 < k < n)$ and $I_{1(t_0)}$ is the ionosphere delay at epoch (t_0). After applying this correction to the observation at epoch $(t_0 + n)$ at eq. (6) we have

$$L_{4(t_{0+n})} - \frac{f_1^2 - f_2^2}{f_1^2} \sum \partial I_{1(t_0,t_{0+n})} = (\lambda_1 N_1 - \lambda_2 N_2) + \frac{f_1^2 - f_2^2}{f_1^2}\left(I_{1(t_0)}\right) + DCBs \tag{15}$$

The epoch-carrier phase Geometry free $L_{4(t_{0+n})}$ at eq. (15) includes two parts, one is due to the spatial and temporal change of the ionospheric delay from epoch (t_0) to $(t_0 + n)$, and another is caused by the change of the signal paths due to the movement of the satellite ambiguity term $(\lambda_1 N_1 - \lambda_2 N_2)$.

5. Elevation and Azimuth Angles and Ionosphere Pierce Point:

To compute elevation and azimuth angle for any satellite, the receiver position in Earth Centered Earth Fixed (ECEF) is converted to geodetic coordinate (λ, φ, z). Then, the satellite position coordinate (x_s, y_s, z_s) from ECEF at the specified epoch is interpolated from the IGS final orbits. The interpolated satellite position is then transformed to a local coordinate frame, East, North, and Up (ENU) system. The transferred ENU is used to calculate elevation and azimuth angles as follows (Dahiraj, 2013 and Sedeek et al, 2017):

$$E = \arctan\left(\frac{x_U}{\sqrt{x_N^2 + x_E^2}}\right) \tag{16}$$

$$A = \arctan\left(\frac{x_E}{x_N}\right) \tag{17}$$

Where: E and A is elevation angle and Azimuth angle of satellite, respectively.

Ionospheric Pierce Point (IPP) location can be computed by providing reference station coordinates (ϕ_r, λ_r), then the geographic latitude and longitude of IPP can be computed according to elevation and azimuth angle of satellite such as follows (Dahiraj, 2013):

$$\psi = \pi / 2 - E' - E \tag{18}$$

Where:

ψ : The offset between the IPP and the receiver;

E' and E: the elevation angles at the IPP and receiver.

$$E' = \sin^{-1}\left(\left(\frac{R_E}{R_E + H}\right)\cos E\right) \quad (19)$$

Where:

R_E: is the mean radius of the spherical Earth (6371 km)

H: is the height of IPP (it is taken to be 450 km)

Usually, the ionosphere assumed to be concentrated on a spherical shell of infinitesimal thickness located at altitude, for example, of 450 km above Earth's surface, i.e., forming single layer model (Rocken et al., 2000). IPP is the intersection point between the satellite receiver line-of-sight, and the ionosphere shell (Figure 1). Slant total electron content (STEC) can be translated into VTEC using Single Layer Model (SLM)

$$VTEC = F(E)\,STEC \quad (20)$$

$$F(E) = \frac{1}{\cos(E')} \quad (21)$$

Where F(E) is the mapping function and E' as mentioned in equation (19).

From equations (11 & 20)

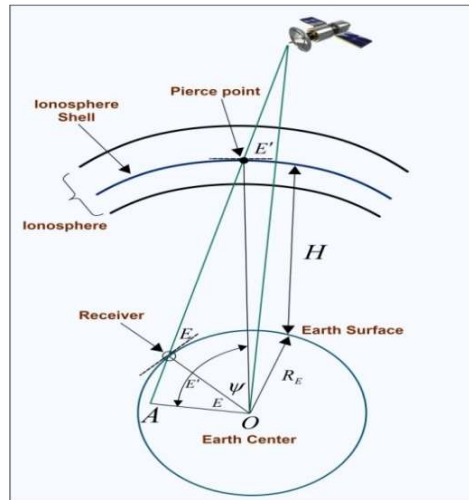$$VTEC = F(E)\frac{I_1 \cdot f_1^2}{40.3} \quad (22)$$

Figure (1): Elements of the spherical ionospheric shell model (Sedeek et al.,2017).

6. Evaluation of the Study

To evaluate the performance of the developed algorithm, TEC maps cover a 24 hours time period at intervals of 2 hours were estimated for observations of Day 98, 2015 for two IGS stations (ANKR, BSHM). ANKR has a geographic Longitude and Latitude

($32.7583°$, $39.8875°$) and BSHM ($35.02°,32.7789°$) respectively as shown in figure (7). A geographic reference frame was used to produce the epoch-specific instantaneous regional maps of the ionosphere. Figure (2) shows the IPP distribution for ANKR station. Figures (4) and (5) show the regional ionosphere maps for both stations using the developed ZDPID code. We use in the current study, the satellite DCB and receiver DCB for the two stations was derived from IGS products (IONEX files).
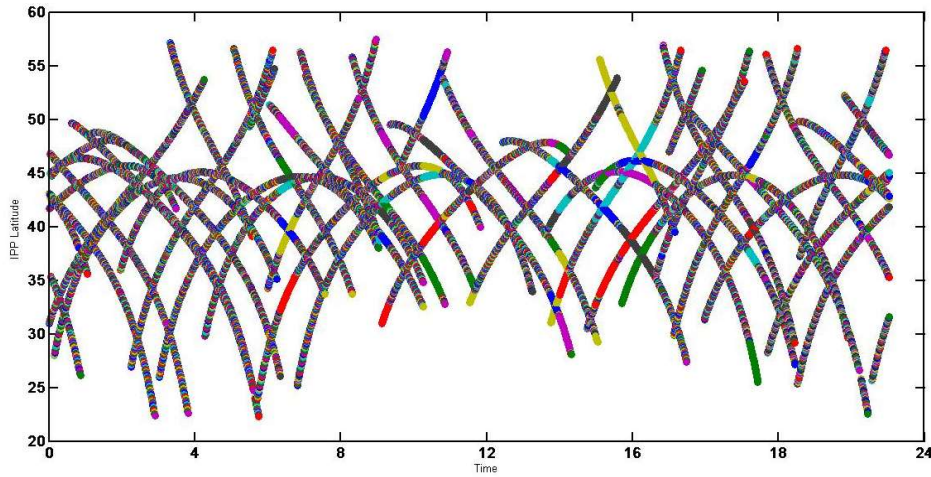

Figure (2).IPP maps for ANKR station of Day 98 (2015).

It should be noted that the IGS GIMs are computed from a Global IGS network, with observation of a combination of ~ 400 permanent GNSS stations. It is observing 4~12 satellites at 30 secretes. This means that more than 250,000 VTEC observations/hour worldwide. It uses Kalman-filter approach with shell model ionosphere with slab centered 450 km. It produces maps for every 2 hours from $180°W$ to $180°$ E with $5°$ spatial resolution in longitude and from $87.5°S$ to $87.5°N$ with $2.5°$ spatial resolution in latitude(Krankowski, 2016). The IGS GIMs are provided by several analysis centers (ACs). We select a region located between $20°~ 45°$north geographic latitude and $20°~ 45°$ longitude. This region covers the IPPs location for most of the processed epochs. The TEC values were interpolated by Kriging method with Surfer software (V.12).We grid the studied region with space $0.5° × 0.5°$ to create high-resolution instantaneous TEC maps (Figure5).

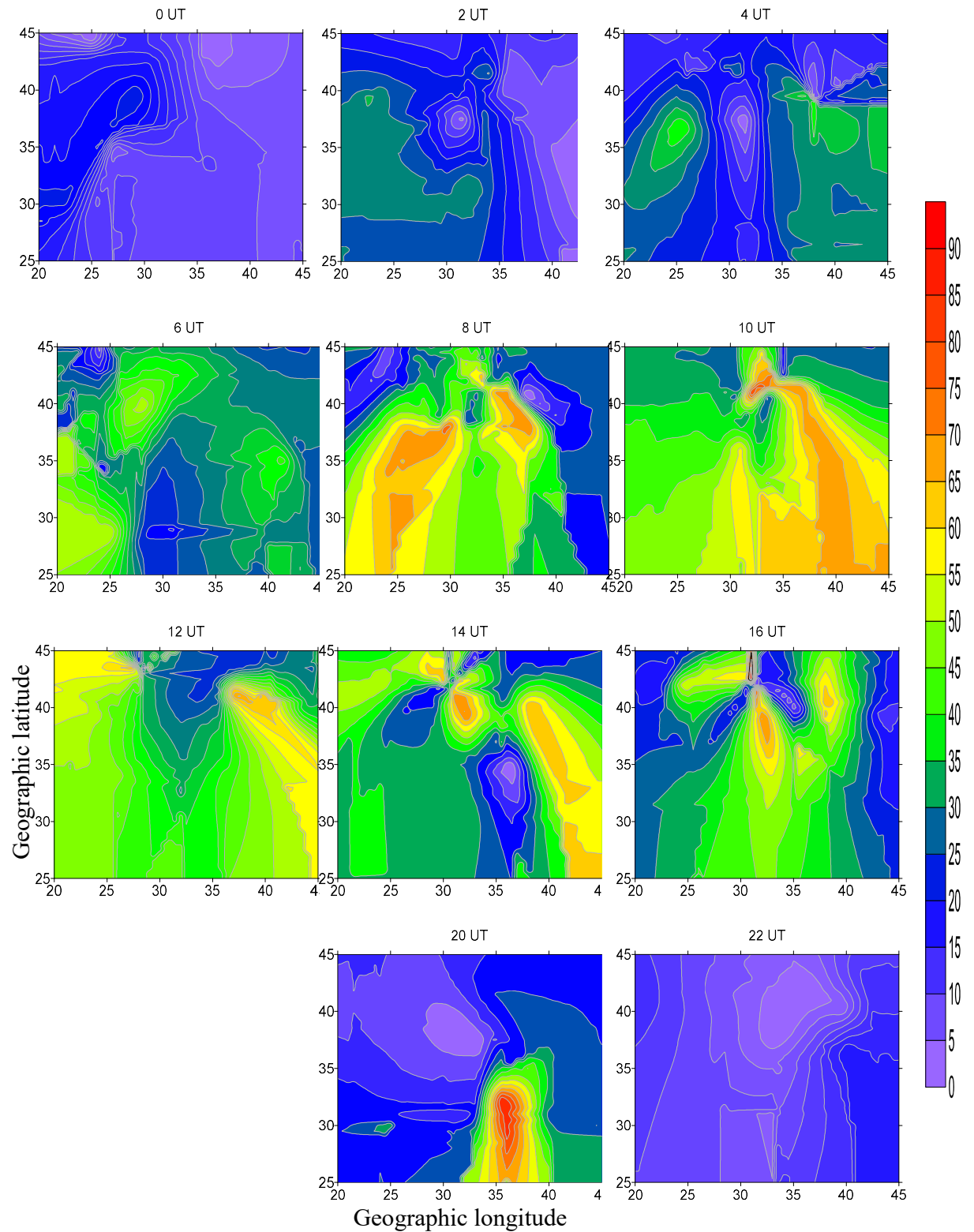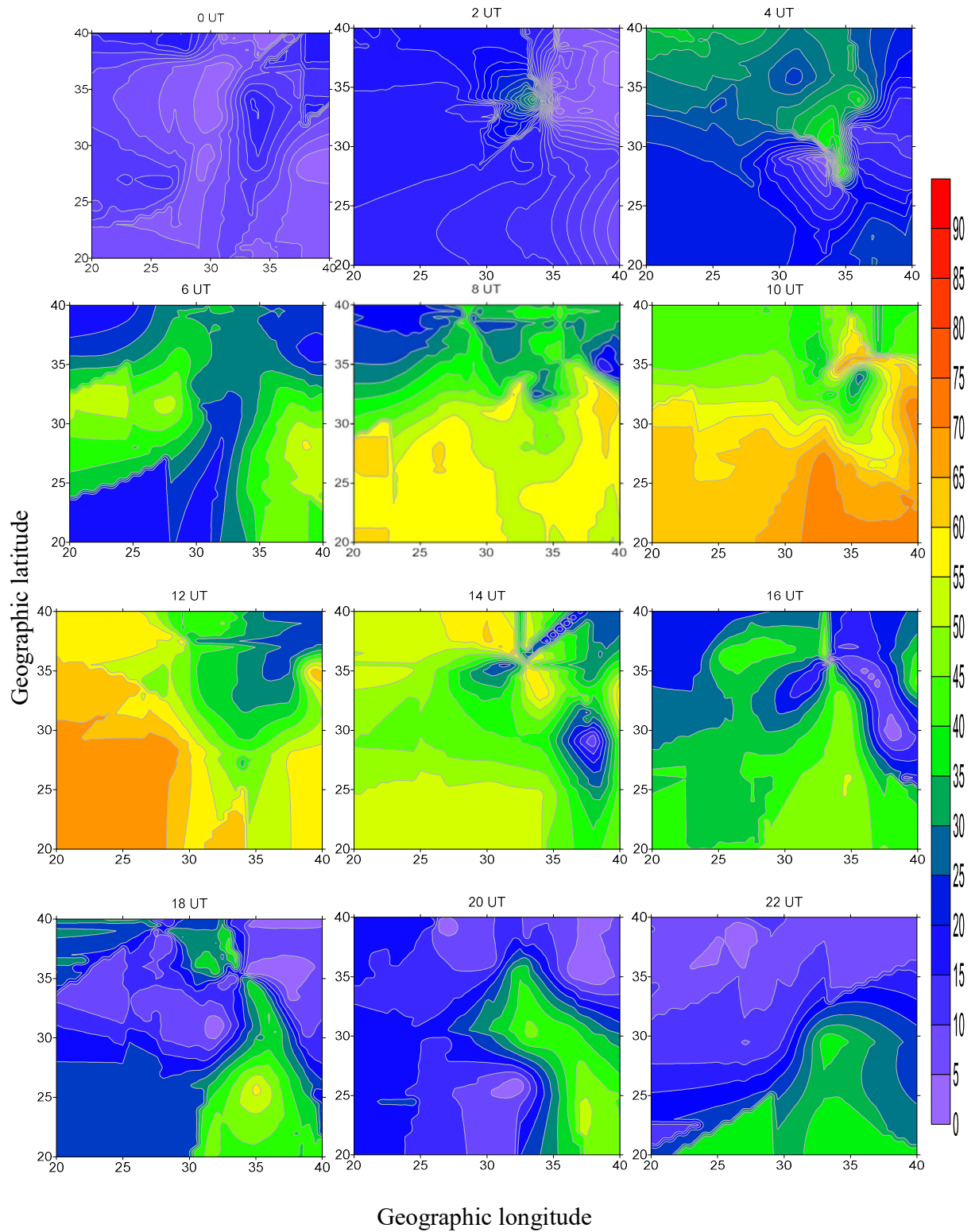Figure (3). TEC maps for ANKR station of Day 98 (2015)

Figure (4). TEC maps for BSHM station of Day 98 (2015).

7. Results and Discussions

The observations of Day 98 (2015) for ANKR, BSHM stations of IGS were used to evaluate the performance of the introduced ZDPID algorithm. In figures (3) and (4) we present the regional ionosphere maps cover a 24 hourly period at intervals of 2 hours for both stations using the developed ZDPID code with cut off angle 10˚. The *TEC* values have been interpolated by Kriging method using Surfer software (V.12) for the selected region located between 20˚~ 45˚N and 20˚~ 45˚ E. As it mentioned before, this region covers the IPPs location for most of the processed epochs. Figure (5) shows *TEC* maps estimated by *GIM* model of day 98 (2015) for a grid of 0.5˚ × 0.5˚ to create high-resolution instantaneous *TEC* maps.

As it is depicted in figure (5), ZDPID gives a much more detailed picture of the local ionosphere map. The IGS GIMs are a combination of TEC derivation from GPS observations, as well as different TEC modeling techniques. This also explains why the TEC derived from GIMs is very smooth over the region. In contrast to the GIMs explains the global nature of GIMs maps. But ZDPID gives real perception of the local ionosphere map.

The obtained mean TEC values every 2 hours of the two IGS stations using the ZDPID are shown in figure (6). As it is shown in the figure, the mean TEC value of IGS GIM is higher than the two stations at the same time. The difference rang between ANKR station and IGS GIM is -2.1 to 3.67 TECU and this rang is -0.29 to 3.65 TECU for BSHM station. We speculate that this may be occurred due to the global nature of IGS-GIM.IGS. Analysis centers (ACs)often use TEC representation algorithms, which result in a model resolution comparable with the whole area of the region under investigation (Schaer, 1999). Wielgosz et al., (2003b) presented an example ionosphere maps for the Ohio CORS compared to the global GIMs. The GIMs general TEC level is higher by about 3-5 TECU, as compared to the maps generated using the Kriging and Multiquadric methods.

Regional ionosphere maps have been generated for both quiet and stormy days by using Bernese 5.0 PPP model by Salih Alcay et al. (2012). They found that the biggest difference between single stations based regional model and GIMs are about 6 TEC in quiet day. Results of our model confirmed that, for regional VTEC maps are generally compatible with GIMs particularly. The GIMs results suffered from the lack of stations at some areas (e.g., over the oceans), e.g. lack of data over the equatorial, North Africa, Atlantic and in-part over equatorial and southern Pacific. This shortage of data, hamper the detection of thee equatorial anomalies (Krankowski, 2016). To overcome this shortage over Egypt and similar territories, the developed algorithm in this paper is applied to improve the temporal and spatial resolution of regional VTEC maps in Egypt.
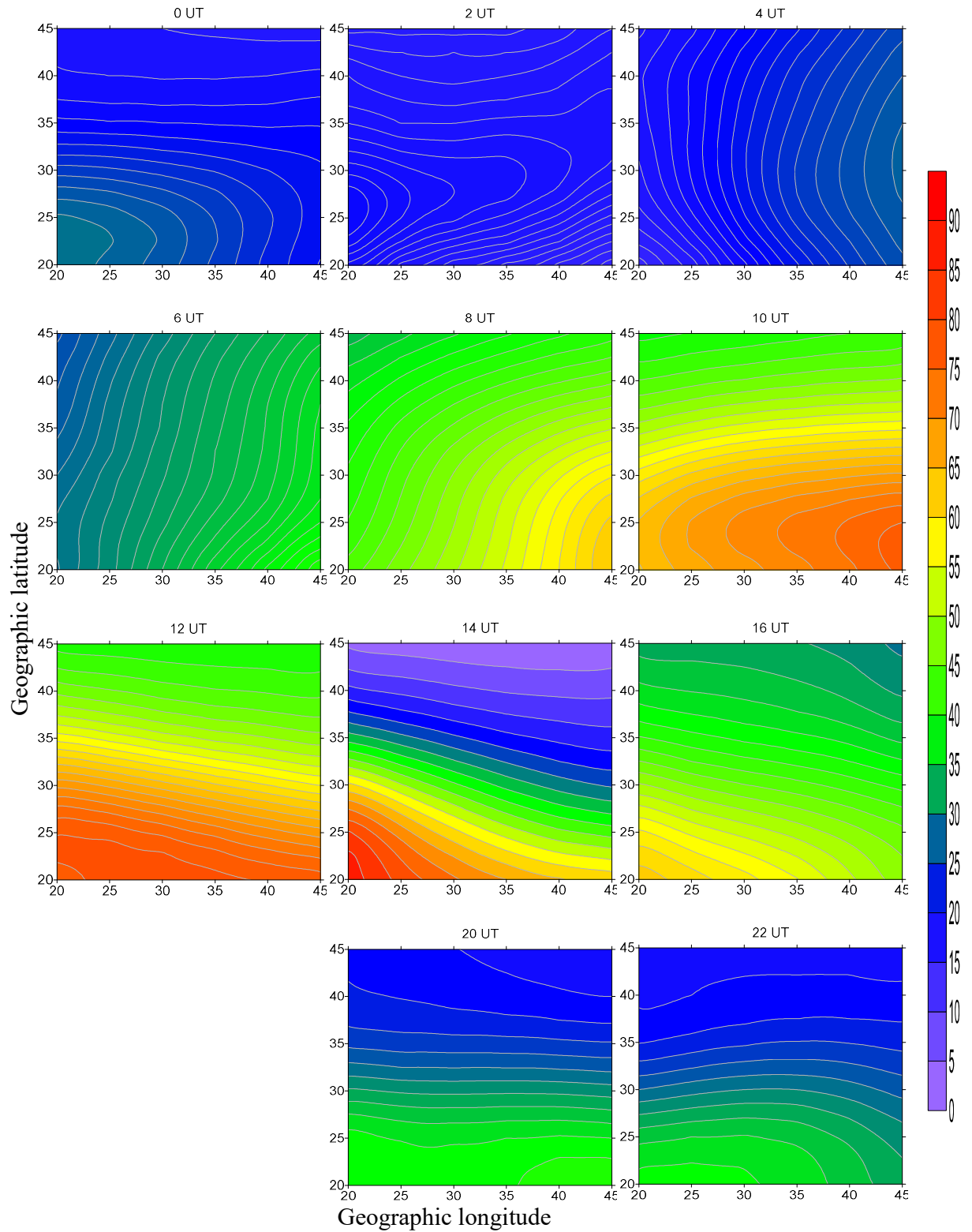
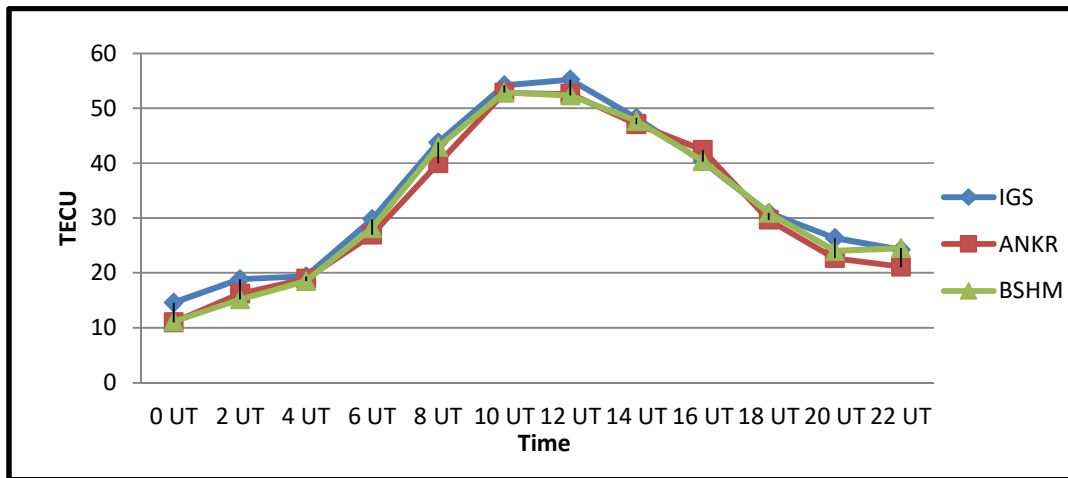Figure (5). TEC maps estimated by GIM model of day98 (2015)

Figure (6).Mean TEC results every 2 hours of the IGS stations and IGS GIMs

This will verify that TEC values could be estimated for three GPS receivers of (BORG, HELW and SAID) observed by NRIAG enclosed the Nile delta (Figure 7). BORG has a geographic Longitude and Latitude (29.5737°, 30.86335°), HELW (31.3434°,29.8616°) and SAID (32.31433°, 31.24569°) respectively.

In the current study, the satellite DCB for the three stations was derived from IGS products (IONEX files) and the receiver DCB was calculated by (Sedeek et al., 2017). Its instantaneous regional TEC maps are drawn on a (0.5° × 0.5° grid) (Figures 8, 9, and 10).

Figure (7).Location of the three Delta Stations, Egypt, and IGS stations used to estimate the regional *TEC* value
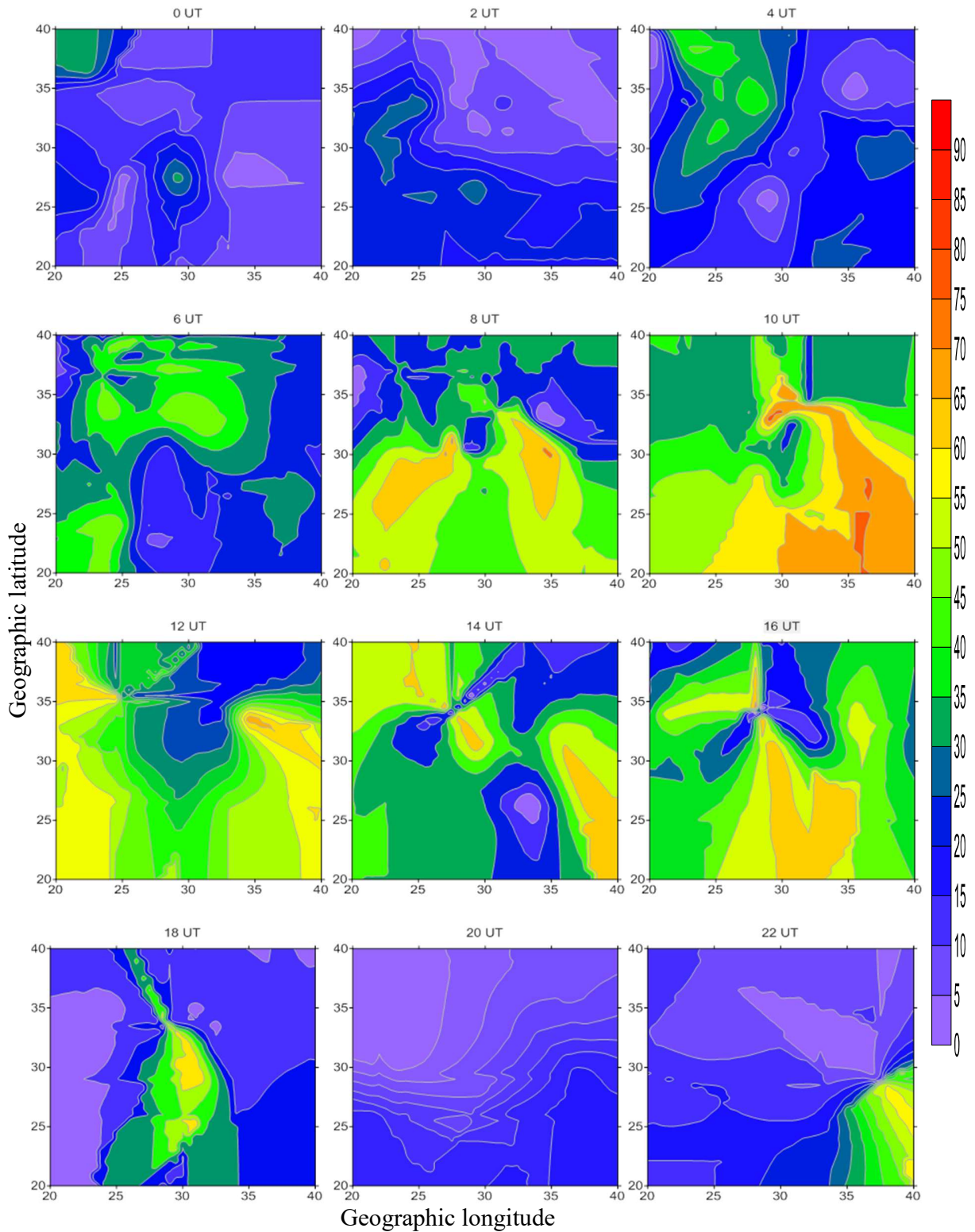
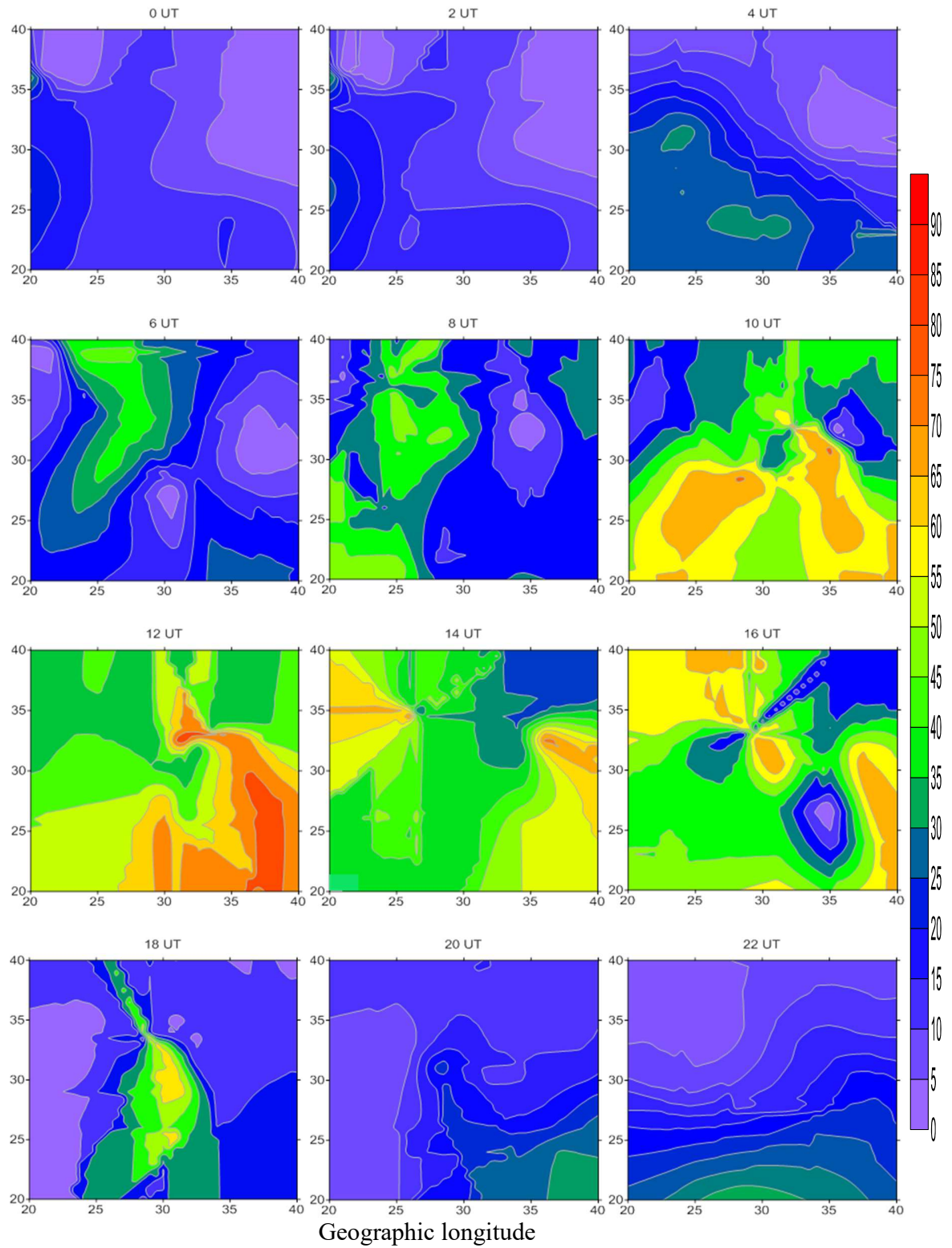Figure (8). TEC maps for BORG station, Day 98-2015

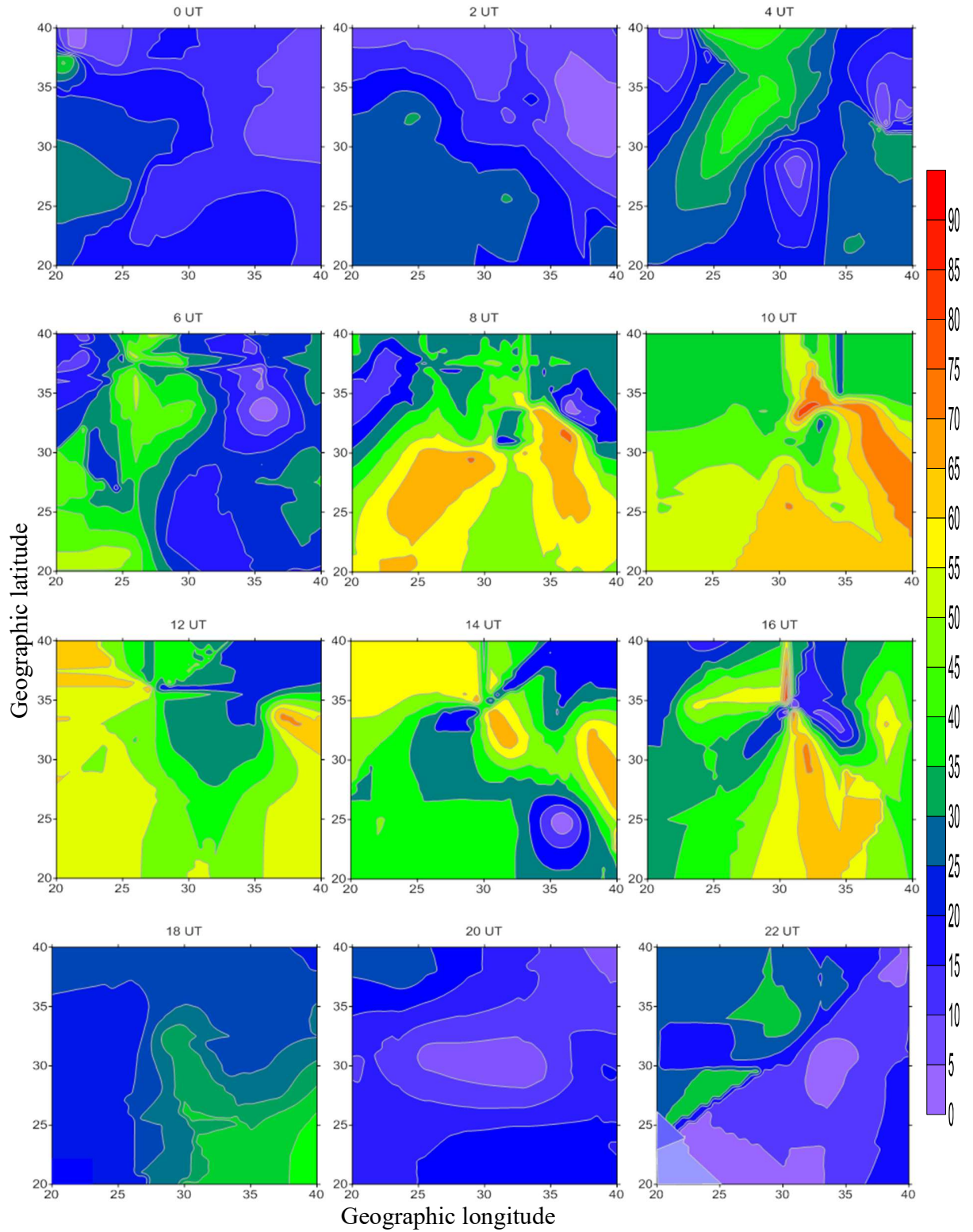Figure (9). TEC maps for HELW station, Day 98-2015

Figure (10). TEC maps for SAID station, Day 98-2015

The mean values for the *TEC* were computed every 2 hours of the three Delta stations and IGS *GIMs*, the results are graphed in Figure (12). As it is seen in the figure, the mean *TEC* value of IGS *GIM* is higher than the three stations at the most time. The difference rang between IGS *GIM* and SAID station is from - 1.1 to 3.69 TECU, from -1.29 to 3.27 TECU for HELW station, and from 0.2 to 4.2 TECU for BORG station. Keep in mind that the GIMs computed results of IGS do not contain any stations from North Africa, and the threshold values used in the comparison are mapped based upon interpolation techniques.
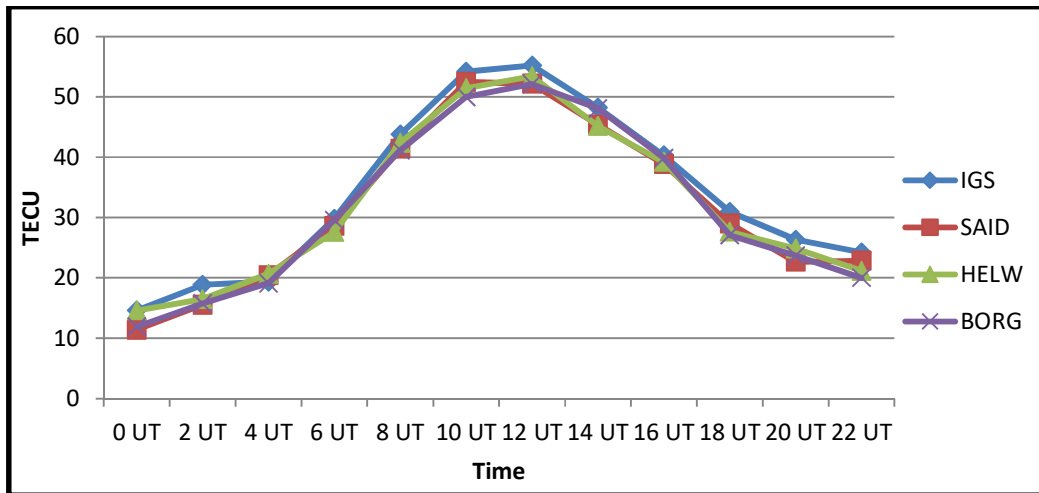

Figure (11).Mean TEC results every 2 hours of the Delta stations and IGS GIMs

8. Conclusions

TEC maps are needed to characterize the ionospheric behavior for satellite based positioning. Many studies have been performed for *TEC* mapping. In the present study a new algorithm based on Zero-differenced phase Ionospheric Delay (ZDPID) is developed. The core of this algorithm is mainly depended on computing the GPS phase ambiguity resolution model by using Sequential Least Square Adjustment. The proposed algorithm has been written using MATLAB code. The computed GIMs of IGS suffered from the lack of stations at some areas (e.g., over the oceans), e.g. lack of data over the equatorial, North Africa, Atlantic and in-part over equatorial and southern Pacific. This shortage of data, hamper the detection of the equatorial anomalies. To overcome this shortage over Egypt and similar regions, and to improve the temporal and spatial resolution of regional *VTEC* maps in Egypt, the new developing algorithm in this study has been applied.

To evaluate the developed algorithm, the *TEC* values have been estimated over two stations from the (IGS), namely ANKR and BSHM. The Global Ionosphere Maps (*GIMs*) were used as a threshold values for comparison with the estimated TEC of the introduced algorithm. To determine the geographical location of the regional maps, coverage circle

concept has been taken into consideration. Obtained results indicated that, for regional vertical TEC maps are generally compatible with GIMs. The mean TEC value of IGS GIM found to be higher than the two stations at the same time. The difference rang between ANKR station and IGS GIM is 0.46 to 3.8 TECU and for BSHM station the difference found to be in the range from 0.1 to 3.65 TECU. ZDPID gives a much more detailed picture and real perception of the local ionosphere map from single point. On the other hand, results of the verification process are clearly shown that the developed algorithm can be successfully used for generating regional ionosphere maps.

9. References:

Araujo-Pradere, E. A., T. J. Fuller-Rowell, P. S. J. Spencer, and C. F. Minter(2007), Differential validation of the US-TEC model, Radio Sci., 42,RS3016, doi:10.1029/2006RS003459.

Ciraolo, L., Azpilicueta, F., Brunini, C., Meza, A., and Radicella S., M., (2007), Calibration errors on experimental Slant Total Electron Content (TEC) determined with GPS, Journal of Geodesy, Vol. 81, No. 2, pp. 111–120.

Dahira jsunehra(2013), Validation of GPS receiver instrumental bias results for precise navigation. Indian Journal of Radio& space Physics, Vol. 42June 2013.pp.175-181.

Deng, Z., M., Bender G. Dick, Ge M., Wickert J., Ramatschi M., and Zou X. (2009), Retrieving tropospheric delays from GPS networks densified with single frequency receivers. Geophysical Research Letters, VOL. 36, L19802, doi:10.1029/2009GL040018.

Feltens, J., J.M. Dow, Martin-Mur T.J., Garcia Martinez C., and Bayona-Perez M.A. (1996), Verification of ESOC Ionospheric Modeling and Status of IGS Intercomparison Activity, In Proceedings of the 1996 IGS Workshop, Silver Spring, MD, 19-21 March, pp. 205-219.

Guochang Xu (2004), GPS Theory, Algorithms and Applications, Library of Congress Control Number: 2007929855. ISBN second edition 978-3-540-72714-9 Springer Berlin Heidelberg New York.

Hofmann-Wellenhof, B., Lichtenegger H., and WalseE. (2008), GNSS Globa lNavigation Satellite Systems; GPS, Glonass, Galileo & more, Springer Wien, New York.

Jakobsen J., Knudsen P., Jensen A.(2010), Analysis of local ionospherictime varying characteristics with singular value decomposition, Journal of Geodesy 85 (7) pages 449456,http://dx.doi.org/10.1007/s00190-010-0378-2.Special Issue on the 43rd ISCIE International Symposium on Stochastic

Jakowski,N., E. Sardon, E. Engler, A. Jungstand, and D. Klln (1996), Relationships Between GPS Signal Propagation Errors and EISCAT Observations, Annales Geophysicae, Vol. 14, pp. 1429-1436.

Komjathy, A. (1997), Global Ionospheric Total Electron Content Mapping Using the Global Positioning System, Ph.D. dissertation, Department of Geodesy andGeomatics Engineering Technical Report No. 188, University of New Brunswick, Fredericton, New Brunswick, Canada, 248 p

Krankowski A., (2016), GPS/TEC Ionosphere diagnostics and IGS, services Space Research Centre of the Polish Academy of Science, 2-3 June 2016.

Langley R.B. (1998), GPS receivers and the observables & Propagation of the GPS signals, GPS for Geodesy, 2nd Ed., Teunissen P.J.G. and Kleusberg A. (Eds.), Springer, Berlin Heidelberg.

Leandro R. F. (2009), Precise Point Positioning with GPS: A New Approach for Positioning, Atmospheric Studies, and Signal Analysis, Ph.D. dissertation, Department of Geodesy and Geomatics Engineering, Technical Report No. 267, University of New Brunswick, Fredericton, New Brunswick, Canada, 232 pp.

Masaharu Ohashi, Taisuke Hattori, Yukihiro Kubo and Sueo Sugimoto(2013), Multi-Layer Ionospheric VTEC Estimation for GNSS Positioning, special Issue on the 43rd ISCIE International Symposium on Stochastic Systems Theory and Its Applications-III Vol. 26, No. 1, pp. 16–24, 2013.

Melbourne W.G. (1985), The case for ranging in GPS based geodetic systems, Proceedings of the 1st international symposium on precise positioning with the global positioning system, Rockville, Maryland, pp 373–386.

Nohutcu, M., Karslioglu, M.O., Schmidt, M. (2010), B-Spline Modeling of VTEC Over Turkey Using GPS Observations, Journal of Atmospheric and Solar-Terrestrial Physics.72 pp.617-624.Systems Theory and Its Applications—III.

Rocken, C., M. Johnson, and J. Braun (2000), Improving GPS surveying with modeled ionospheric corrections", Geophys. Res. Lett., 27, 3821–3824.

Salih Alcay, CemalOzer Yigit, CevatInal (2012), GPS Based Ionosphere Mapping Using PPP Method, FIG Working Week 2012Knowing to manage the territory, protect the environment, evaluate the cultural heritage Rome, Italy, 6-10 May 2012.TS09B - Precise Point Positioning, 5618 1/11.

Sardon, E., and Zarraoa, N. (1997), Estimation of total electron-content using GPS data: how stable are the differential satellite and receiver instrumental biases?, Radio Science, Vol. 32, pp. 1899–1910.

Sardon, E., N. Jakowski, and N. Zarraoa (1995), Permanent Monitoring of TEC Using GPS Data: Scientific and Practical Aspects., EOS Transactions of the American Geophysical Union, Vol. 76, No. 17, Supplement, p. 87 (abstract).

Schaer, S. (1999), Mapping and Predicting the Earth's Ionosphere Using the Global Positioning System, PhD dissertation, Astronomical Institute, University of Berne, Switzerland, pp. 205.

Sedeek A. A., Doma M. I., Rabah M. and Hamama M. A. (2017), Determination of Zero Difference GPSDifferential Code Biasesfor Satellites and Prominent Receiver Types, Arabian journal of geosciences, vol. 10, January 2017.

Stanislawska, I., Juchnikowski, G., Hanbaba, R., Rothkaehl, H.,G. Sole, and Z. Zbyszynski (2000), COST 251 Recommended Instantaneous Mapping Model of Ionospheric Characteristics – PLES, Phys. Chem. Earth (C), vol. 25, no. 4, pp. 291-294.

Wielgosz P., L.W. Baran, I.I. Shagimuratov and M.V. Aleshnikova (2003a), Latitudinal variations of TEC over Europe obtained from GPS observation, accepted by Annales Geophysicae.

Wielgosz, P., Grejner- Brzezinka, D. and Kashani, I. (2003b), Regional Ionosphere Mapping with Kriking and Multiquadric Methods, Journal of Global Positioning Systems, vol. 2, no. 1, pp 48-55.